

# Comparison between topographic and photogrammetric techniques for deformation monitoring of the dome of the Massimo Theatre in Palermo

Gino DARDANELLI, Pietro ORLANDO and Benedetto VILLA, Italy

**Key words:** Deformations monitoring, Thermal dilatation, Robotic total station, Digital photogrammetry, Thermal imaging camera.

## Summary

*This paper shows the first results of a study aimed at monitoring the deformations of the dome of the Massimo Theatre in Palermo caused by thermal dilatations, with the use of topographic and photogrammetric integrated techniques. Particularly, two robotic total stations and high precision digital photogrammetric systems were employed. In order to correlate the displacements of the rollers on which the steel structure of the dome rest with the thermal gradients, different thermal images were acquired by a thermal imaging camera. The main goal of the work was to compare the two techniques with reference to very small (submillimeter) deformation measurements. The obtained results show that the rollers are still working correctly. In fact, for a thermal gradient of 6 °C both topographic and photogrammetric techniques determined displacements in the order of 0.8 mm, according with the expected deformations of the theoretical model.*

# Comparison between topographic and photogrammetric techniques for deformation monitoring of the dome of the Massimo Theatre in Palermo

Gino DARDANELLI, Pietro ORLANDO and Benedetto VILLA, Italy

## 1. INTRODUCTION

The measurement of displacements and deformations has always been object of interest from geodesy and classic topography. In the last years, the field of surveying has undergone a deep change because of the wide spread of electronics and informatics. New instruments and methods have been produced, more and more fast, automatic, reliable; suffice it to consider GPS, robotic total stations (RTS), digital photogrammetric and laser-scanning techniques. The field of structures monitoring has particularly taken advantage of this change. In this regard, for example, RTS are of great use, allowing to carry out control measurements without the presence of the surveyor.

This paper outlines the first results of a research work, carried out within an interdisciplinary collaboration at the Department of Civil, Environmental and Aerospace of Palermo University, directed towards the deformations monitoring of the dome of the Massimo Theatre in Palermo, caused by thermal dilatations, with the use of topographic and photogrammetric techniques.

The Massimo Theatre (fig. 1), built as from 1873 on G.B. Filippo Basile's design, is the biggest opera house in Italy and one of the largest of Europe. Its dome, having radius of 27.3 m, is supported by 16 steel ribbings resting on mobile rollers located on a 1.1 m wide masonry curb (figg. 2, 3).



Figure 1 - Aerial photo of the Massimo Theatre with the dome in the centre



Figure 2 - Interior view of the dome



Figure 3 - Connection between ribbings and curb

The rollers, formed by a mobile part moving inside of a fixed slot (fig. 4), serve to absorb the dilatations of the steel ribbings, produced by thermal gradients occurring in the space of a day and in the succession of the seasons, so avoiding the creation of strains on the structure. The goal of the research work also was to verify the efficiency of the rollers, after over one century from its making.

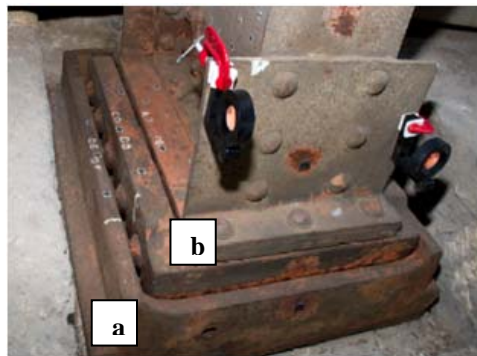


Figure 4 – Detail of the roller a) fixed part b) mobile part

## 2. TOPOGRAPHIC SURVEY

As regard the topographic method, two Trimble S8 RTS were used (fig. 5), centered over a precision trivet located on two diametrically opposed points of the curb ( $S_1$  and  $S_2$ ). Before monitoring operations began, some laboratory tests were carried out, directed to verify the measurements accuracy, reported in the instrument technical specifications, equal to  $\pm 1''$  for angles and to  $\pm(1\text{mm} + 1\text{ppm})$  for distances. Two mini-prisms were located at a distance of about 30 m, repeating the measurement of angular directions and distances a hundred times. This test enabled to determine the effective accuracy; for distances the expected value was confirmed, for angles a value equal to  $\pm 3''$  was determined. Monitoring operations regarded 6 rollers out of 16, identified by increasing codes from C1 to C6; two mini-prisms were located on each roller, to enable the observation from both station points. Besides another mini-prism was placed on an outside fixe point (F), not influenced by the thermal dilatations of the ribbings.



Figure 5 - Trimble S8 RTS

So it was possible to determine the absolute displacements with respect to an exterior reference system, beside the relative ones among the points under control.

Figure 6 shows the graph of the points involved in monitoring. In the space of a day six series of measurements were carried out, one every four hours. To improve the angular accuracy, measurements were reiterated 10 times, calculating this number by the expression

$$n = \sigma^2 / \sigma_m^2$$

where  $\sigma^2$  is the variance of measurements system and  $\sigma_m^2$  is the variance of the mean of measurements.

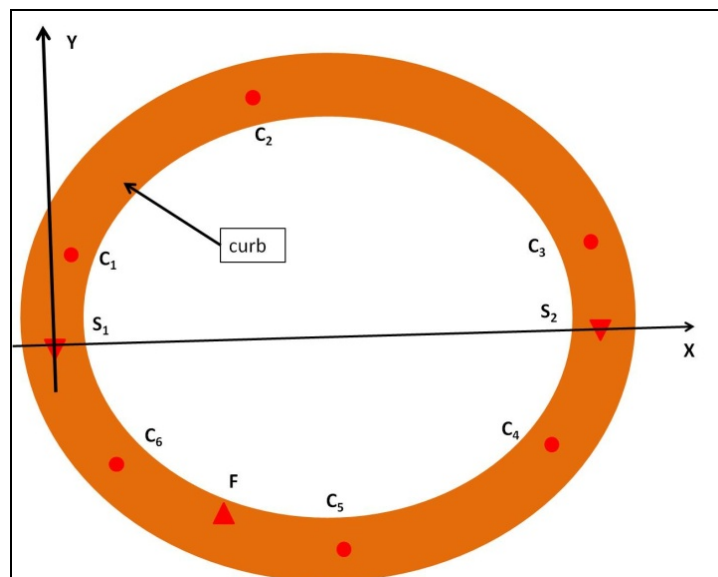


Figure 6 - Scheme of the survey and reference system

Whereas the expected horizontal displacements, in accordance with the theoretical model provided by structural engineers, were in the order of  $0.7\div 0.8$  mm, and the farther point was at a distance of about 27 m, the value of the angle subtended to the expected displacement was calculated and its accuracy ( $\sigma_m^2$ ) was determined, assuming it equal to one order of magnitude smaller than the measurement.

From each of two point stations angle and distance parameters related to the other point station, to the six control points on the rollers and to the fixed point were determined. Altogether 1200 values of directions, vertical angles, slope distances were acquired. At each series of measurements, for each control point, eliminated outliers identified previously, mean values of horizontal and vertical angles, of slope distances were determined and then the coordinates, with related accuracy, were calculated. In this regard a local reference system was established, with origin on the point  $S_1$ , X axis passing through point  $S_2$  and Z axis directed upwards.

Table 1 reports, as an example, for the six series of measurements, data related to the point  $C_1/S_1$  (concerning the roller  $C_1$  observed by the station  $S_1$ ). Table 2 reports instead the coordinates of the points  $C_3/S_1$  and  $C_3/S_2$ , related to the roller  $C_3$  observed by the points  $S_1$  and  $S_2$ , respectively; high correlation of the obtained values denotes the reliability of the acquired measurements.

From the values of the coordinates the differences  $\Delta X$ ,  $\Delta Y$ ,  $\Delta Z$ , i.e. horizontal and vertical displacements, were computed at each series of measurements. Figures 7 and 8 illustrate the displacements of the points  $C_1/S_1$ ,  $C_3/S_1$  and  $C_3/S_2$  along the coordinate axes and the whole horizontal displacement; it may be noticed that vertical component of displacement is quite absent; besides remarkable concordance between the points belonging to the same roller is confirmed.

$C_1/S_1$	Time	Hz. direction	Vert. angle	Slope dist.	X	Y	Z
	9.04.22	273.78712	106.12622	1.7527	100.5065	101.6695	9.8316
	13.17.22	273.79217	106.12724	1.7525	100.5065	101.6692	9.8316
	17.30.24	273.79201	106.1270	1.7524	100.5065	101.6691	9.8316
	21.43.26	273.79349	106.12768	1.7522	100.5065	101.6689	9.8316
	1.56.24	273.79238	106.12738	1.7526	100.5066	101.6693	9.8316
	7.55.57	273.78678	106.12565	1.7525	100.5064	101.6693	9.8316

Table 1 - Point  $C_1/S_1$  data

$C_3/S_1$	Time	X	Y	Z	$C_3/S_2$	Time	X	Y	Z
	9.04.22	126.1065	103.1575	9.9093		9.04.22	126.2273	103.2133	9.9086
	13.17.22	126.1066	103.1575	9.9092		13.17.22	126.2274	103.2131	9.9086
	17.30.24	126.1063	103.1578	9.9092		17.30.24	126.2272	103.2133	9.9086
	21.43.26	126.1063	103.1574	9.9092		21.43.26	126.2271	103.2132	9.9086
	1.56.24	126.1062	103.1572	9.9093		1.56.24	126.2269	103.2132	9.9086
	7.55.57	126.1063	103.1574	9.9093		7.55.57	126.2271	103.2132	9.9087

Table 2 - Coordinates (in meters) of the control points  $C_3/S_1$  and  $C_3/S_2$

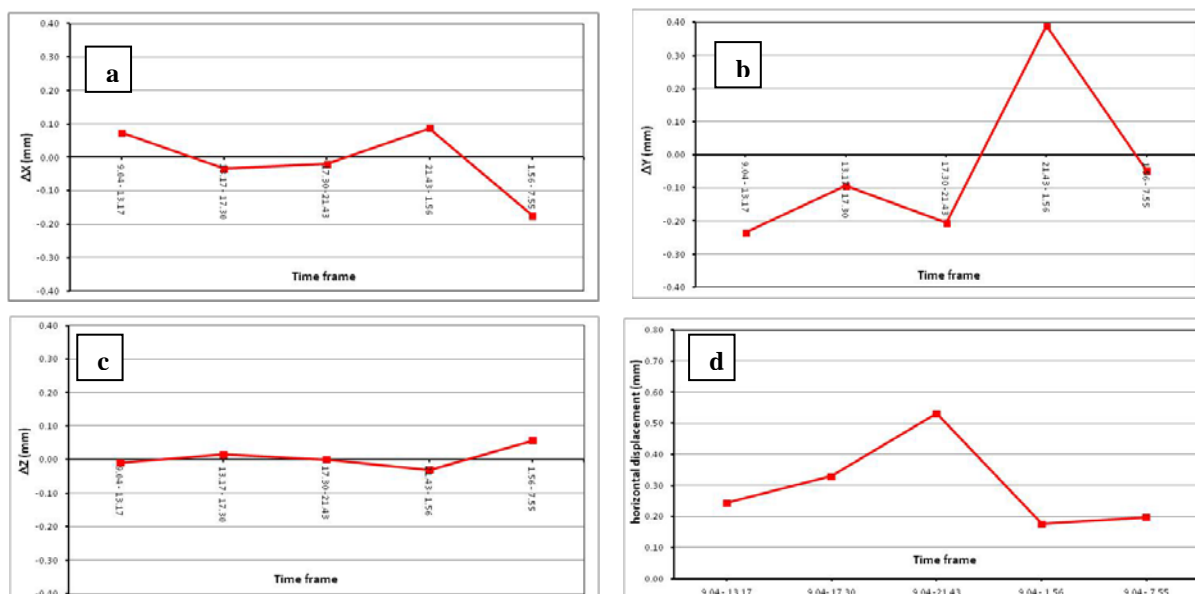


Figure 7 - Displacement of the point C<sub>1</sub>/S<sub>1</sub> a) ΔX b) ΔY c) ΔZ d) horizontal displacement

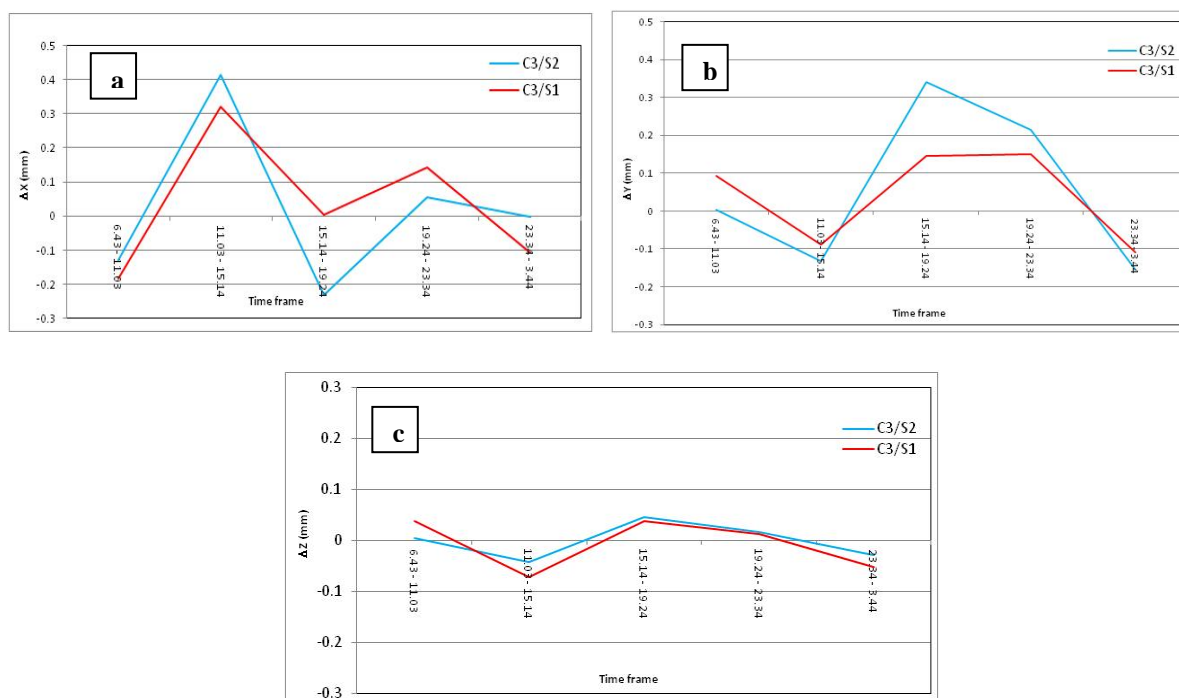


Figure 8 - Displacement of the points C<sub>3</sub>/S<sub>1</sub> (in red) and C<sub>3</sub>/S<sub>2</sub> (in blue) a) ΔX b) ΔY c) ΔZ

### 3. PHOTOGRAMMETRIC SURVEY

Monitoring by photogrammetric techniques was possible to do only of two rollers (C<sub>1</sub> and C<sub>3</sub>). For taking photos, Canon Eos-01 Mark II digital camera with 50 mm focal



length was used, mounted on a slide (fig. 9). The camera axis was directed downwards, therefore operating procedure was similar to the one typical of the aerial photogrammetry. Some circular photogrammetric targets (denoted by the letters  $D_i$ ), then used as tie-points, were placed on the upper surface of the rollers. Four stereopairs of photos of the two rollers were taken in the space of a day, at 10, at 2 p.m., at 3.30 p.m. and at 6 p.m. (fig. 10).



Figure 9 - Canon Eos-01 Mark II digital camera



Figure 10 - Stereopairs of photos of the roller  $C_1$  a) 2 p.m. b) 6 p.m.

The object distance was calculated with respect to the accuracy of the coordinates of the object point by the relationships

$$\sigma_x = \sqrt{m_b^2 \sigma_{\xi}^2 + \left( \frac{\xi_l}{c} m_b \frac{Z}{B} \right)^2 \sigma_{P_{\xi}}^2}$$

$$\sigma_y = \sqrt{m_b^2 \sigma_{\eta}^2 + \left( \frac{\eta_l}{c} m_b \frac{Z}{B} \right)^2 \sigma_{P_{\xi}}^2}$$

$$\sigma_z = m_b \frac{Z}{B} \sigma_{P_{\xi}}$$

where

- $c$  is the camera focal length
- $Z$  is the object distance
- $B$  is the baseline
- $m_b = Z/c$  is the inverse of the average photo scale
- $\xi_l, \eta_l$  are the coordinates of the image point
- $\sigma_{\xi}, \sigma_{\eta}$  are the standard deviations of the image points coordinates
- $\sigma_{P_{\xi}}$  is the standard deviation of the parallax  $P_{\xi}$

Having established the baseline equal to the maximum range of the slide (about 7 cm), known the camera focal length, the resolution and the size of the sensor, and assumed sub-pixel values (verified afterwards) for tangential parallax, the maximum object distance resulted equal to 65 cm. Also in this case the analysis of photogrammetric data was directed to determine the trend of the tie-points coordinates during the day and to consider the compliance of the achieved results with the available structural model.

Data processing was organized into following four steps:

- 1) camera calibration to remove radial and tangential distortions;
- 2) interior and exterior orientation of the stereopairs;
- 3) calculation of the tie-points coordinates;
- 4) analysis of the coordinates trend during the day.

The calibration was carried out by means of a grid, formed of points and shapes of known coordinates (fig. 11); the photos of the grid were taken at a distance equal to the one used during the monitoring operations so that the same conditions of focalization were reproduced.

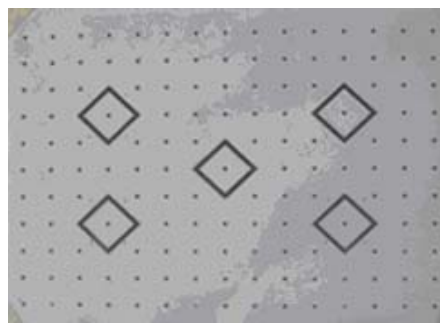


Figura 11 - Calibration grid



*Pi-Calib* software was used to obtain the values of the seven unknown parameters (focal length; x, y coordinates of the principal point; two coefficients related to radial distortion; two coefficients related to tangential distortion) necessary for the interior orientation (tab. 3).

The three following steps of data processing were carried out through Topcon *Image Master* software, usually used to extract point cloud models from stereopairs and characterized by powerful image-matching and bundle adjustment algorithms, necessary to obtain a submillimeter accuracy.

Camera focal length	49.6701 mm
Xpp	16.4184 mm
Ypp	10.728 mm
pixel size (x)	0.0065 mm
pixel size (y)	0.0665 mm

Table 3 - Parametrs of the interior orientation

Relative and absolute orientation, procedure of primary importance to obtain the required accuracy, was carried out using, as tie-points and control points, circular targets suitably designed. Tie-points were located both on the fixed part of the roller and on the one mobile (fig. 12). The exterior reference system was established by a grid on which control points having known coordinates were set out on two rows, identified by the letters A and B, respectively (fig.13).

*Pi-Calib* identifies, through image-matching algorithms, the centre of targets concerning tie-points and control points in a semiautomatic way, independently of ability of the photogrammetric operator. Three of the control points were considered as check points (fig. 14) and its coordinates were determined. Comparison between these last coordinates and ones known enabled to calculate the differences which came out of a smaller order of magnitude than the required accuracy.

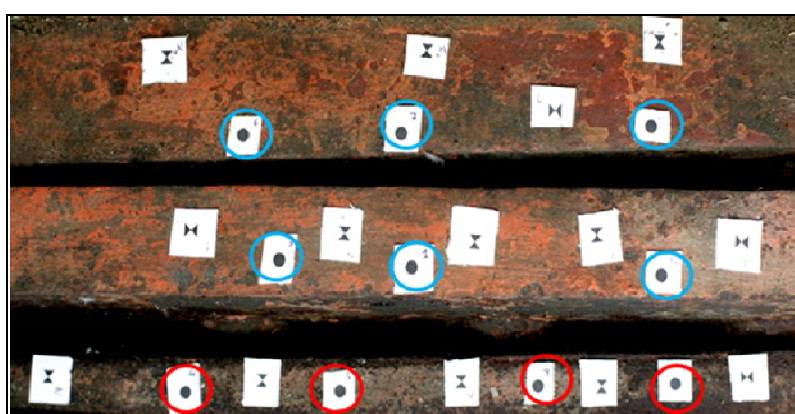


Figure 12 - Tie-points: fixed part (in red), mobile part (in blue)

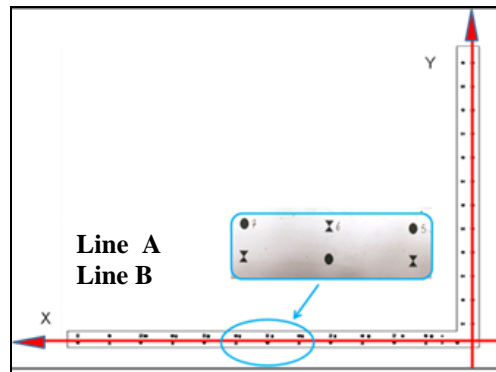


Figure 13 - Grid of the control points

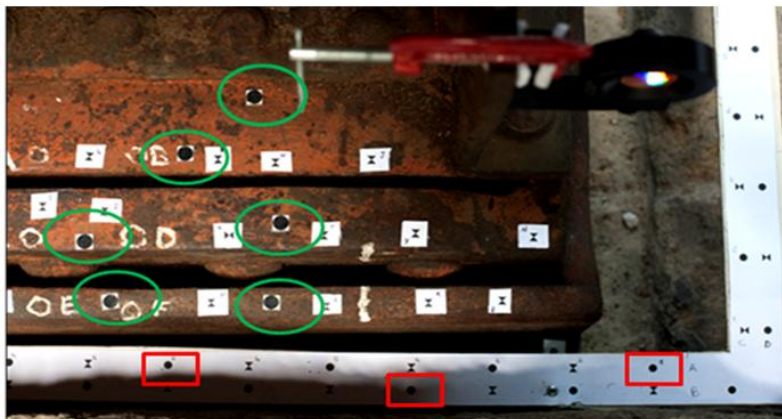


Figure 14 - Tie-points (in green), check points (in red)

Points	2.30 p.m.					
	Tie-Points Y-parallax			Coordinates		
	Point	y-prx [pixel]	y-prx[mm]	X[m]	Y[m]	Z[m]
Control points	3	0.02	0.0116	0.02	0.15	0
	4	0.01	0.055	0.00	0.20	0
	5	-0.16	-0.01033	0.02	0.25	0
	6	0.31	0.1988	0.00	0.30	0
	7	-0.01	-0.0064	0.02	0.35	0
	8	0.05	0.0354	0.00	0.40	0
	9	-0.01	-0.0074	0.02	0.45	0
Tie-Points	D05	-0.16	-0.01056	0.0561	0.2524	0.0108
	D06	-0.09	-0.0597	0.0549	0.3497	0.0136
	D04	-0.05	-0.0356	0.0962	0.2257	0.0567
	D01	-0.02	-0.0125	0.0945	0.3417	0.0598
	D07	-0.02	-0.0129	0.1416	0.358	0.0583
	D02	0.13	0.0856	0.1443	0.2625	0.0558

Table 4 - Parallax and absolute coordinates of tie-points (2.30 p.m.)

Tables 4 and 5 report the parallaxes coming out from the relative orientation. All the values result sub-pixel in compliance with the initial hypothesis of the photogrammetric survey planning. On the table 6 the coordinates and the displacements of the points D01 and D06 are reported, with regard to the four stereopairs; figure 13 shows the trend of the displacements  $\Delta X$  and  $\Delta Y$  of the same points, during the three time frames. As it was to be expected, point D06, located on the fixed part of the roller, had displacements much smaller than ones of the point D01.

Points	6 p.m.					
	Tie Points Y-parallax			Coordinates		
	Point	y-prx [pixel]	y-prx[mm]	X[m]	Y[m]	Z[m]
Ground Control Points	3	-0.04	-0.0284	0.015	0.15	0
	4	0.04	0.0284	0	0.2	0
	5	-0.07	-0.0469	0.015	0.25	0
	6	0.08	0.0511	0	0.3	0
	7	-0.05	-0.0316	0.015	0.35	0
	8	0.22	0.01441	0	0.4	0
	9	-0.23	-0.01488	0.015	0.45	0
Tie Points	D05	-0.02	-0.011	0.0561	0.2522	0.0116
	D06	0.01	0.044	0.0549	0.3495	0.015
	D04	-0.08	-0.0492	0.0962	0.2253	0.0575
	D01	0.01	0.071	0.0945	0.3413	0.0613
	D07	0.08	0.0501	0.1417	0.3576	0.06
	D02	0.06	0.0415	0.1444	0.2622	0.0568

Table 5 - Parallax and absolute coordinates of tie-points (6 p.m.)

D01 Coordinates				D06 Coordinates			
	X (m)	Y (m)	Z (m)		X (m)	Y (m)	Z (m)
2 p.m.	0.0945	0.3417	0.0598	2 p.m.	0.0549	0.3497	0.0136
6 p.m.	0.0945	0.3413	0.06	6 p.m.	0.0549	0.3495	0.0138
10 a.m.	0.0941	0.3406	0.0621	10 a.m.	0.0547	0.3492	0.0144
3.30 p.m.	0.0943	0.3407	0.0619	3.30 p.m.	0.0548	0.3493	0.0139
Time frame	Displacements			Time frame	Displacements		
	$\Delta X$ (mm)	$\Delta Y$ (mm)	$\Delta Z$ (mm)		$\Delta X$ (mm)	$\Delta Y$ (mm)	$\Delta Z$ (mm)
2 - 6	0.011	-0.457	0.174	2 - 6	0.036	-0.16	0.148
6 - 10	-0.431	-0.667	2.098	6 - 10	-0.188	-0.294	0.659
10 - 3.30	0.271	0.152	-0.155	10 - 3.30	0.118	0.082	-0.529

Table 6 - Coordinates and displacements of tie-points D01 and D06

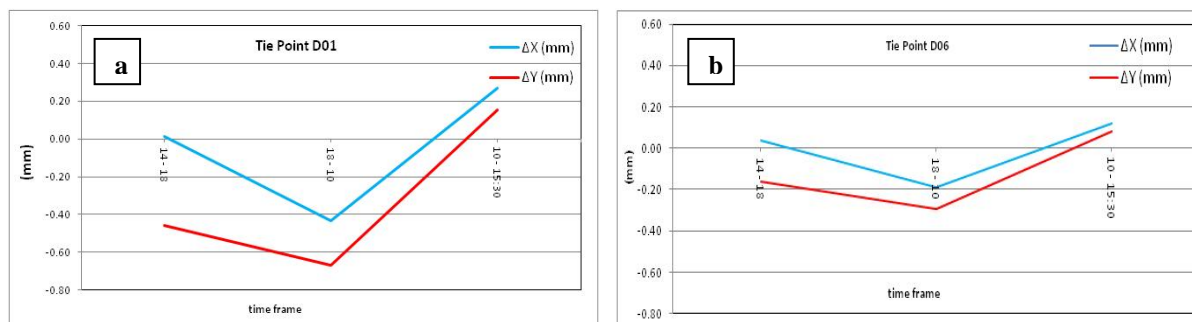


Figure 13 - Displacement of tie-points a) D01 b) D06

#### 4 THERMAL DATA

In order to correlate the displacements of the rollers with the dilatations produced by steel thermal gradients, three thermal images were acquired by *Flucke TiR 32* thermal imaging camera (fig. 14) at the same time as topographic and photogrammetric survey, and precisely at 10 a.m., at 3 p.m. and at 8 p.m.. Thermal images show that during the day steel is subject to thermal gradients of about 6°C (fig. 15). This data, used as input for the theoretical structural model, enabled to verify the accordance of the measured displacements with the ones expected, considering that the theoretical model, for each degree of thermal variation, expected displacements equal to 0.12 mm.



Figure 14 - *Flucke TiR 32* thermal imaging camera

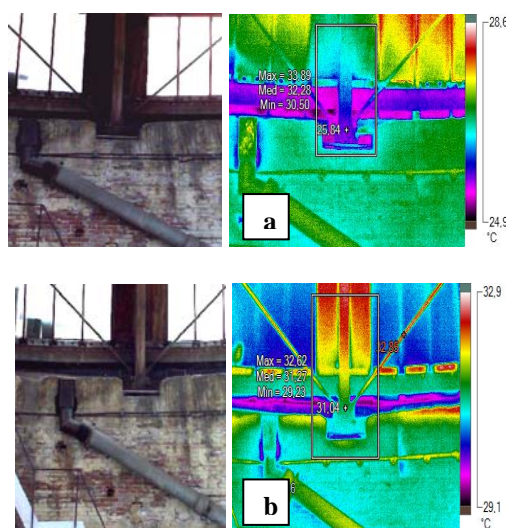


Figure 15 - Thermal images of the roller C1 a) at 10 a.m. b) at 8 p.m.

## 5 CONCLUSIONS

Planning of topographic and photogrammetric survey was directed to obtain random errors of one order of magnitude smaller than the expected displacements; in fact, if errors had been of the same order of magnitude or even greater than one of the possible displacements, it couldn't discriminate the displacements from measurement errors.

The results obtained at the end of this first phase of the research work outline almost exclusively the horizontal component of the displacements; as it was expected, the vertical component is practically equal to zero. Displacements determined by topographic techniques, besides, are of the same size of the ones determined by photogrammetric techniques and for both methods the mean value of the absolute displacements of the rollers results practically identical, equal to about 0.8 mm. This result, quite in accordance with previsions of the theoretical model, demonstrates, on the one hand, that until today the rollers accomplish its task very well; on the other side, that both techniques, topographic and photogrammetric, obviously if used in the proper way, are absolutely suitable to determine submillimeter displacements.

Topographic methods have two substantial advantages over the photogrammetric ones; the former consists in a complete automation of the measurements acquisition, apart from the initial cycle which requires necessarily manual intervention, the latter in the rapidity of data processing; in fact robotic instrument is usually equipped with a software able to provide quickly coordinates, statistical parameters of the measurements and displacements. Instead the strong point of the photogrammetric techniques is connected especially with the cost of instrumentation, considerably lower than the one necessary for topographic survey; on the other side, data processing (orientation and restitution of the coordinates) requires longer time and greater problem solving power.

## REFERENCES

- Amini, A. Sh., Varshosaz, M., and Saadatseresht, M. (2008). Deformation determination of aircraft parts by photogrammetry. *The International Archives of the Photogrammetry, Remote Sensing and Spatial Information Sciences*. Vol. XXXVII. Part B5. Beijing 2008, 135-138.
- Barazzetti, L., and Scaioni, M. (2008). Metodi fotogrammetrici per la misura delle deformazioni nelle prove sui materiali da costruzione. *Atti della 12a Conferenza Nazionale Asita*, 263-268.
- Brigante, R., Dominici, D., Fastellini, G., Radicioni, F., and Stoppini, A. (2009). Confronto e integrazione fra tecniche geomatiche per la documentazione e il monitoraggio dei beni culturali. *Atti della 13<sup>a</sup> Conferenza Nazionale Asita*, 537-542.
- Coppa, U., Guarnieri, A., Pirotti, and F., Vettore, A. (2008). Integrazione di tecniche di rilevamento per il controllo di stabilità di una struttura storica. *Atti del Convegno Nazionale Sifet*, 174-181.



Dominici, D., Fastellini, G., Radicioni, F., and Stoppini, A. (2008). An integrated monitoring system for the monumental walls of Amelia. Proceeding of the 13<sup>th</sup> FIG Symposium on Deformation measurement and Analysis.

Grassi, S., Radicioni, F., and Stoppini, A. (2003). Monitoraggio tridimensionale in tempo reale delle deformazioni: Prove in condizioni operative su una stazione totale automatica di alta precisione. Atti della 13<sup>a</sup> Conferenza Nazionale Asita, 1233-1238.

Grussenmeyer, P., Landes, T., Voegtli, T., and Ringle, K. (2008). Comparison methods of terrestrial laser scanning, photogrammetry and tacheometry data for recording of cultural heritage buildings, The International Archives of Photogrammetry and Remote Sensing, Vol. XXXVII, part B5, 213-218.

Henriques, M. J., Mateus, P. B., Palma, P., and Cruz, H. (2008). Modelling the behaviour of a large span glulam arch of Atlântico Pavillion, Proceeding of the 13<sup>th</sup> FIG Symposium on Deformation measurement and Analysis.

Junga, S. H., Yua, J. H., Leeb, J. K., and Gea, L. (2008). Automatic modelling method for steel structures using photogrammetry, Int. Archives of Photogrammetry and Remote Sensing, Vol. XXXVII, part B5, 169-174.

Kasser, M., and Egels, Y. (2002). Digital Photogrammetry, Taylor & Francis.

Kraus, K. (1997). Photogrammetry Vol. 1 & Vol. 2, Advanced Methods and Applications, Levrotto & Bella Ed., Dummer/Bonn.

Linder, W. (2003). Digital Photogrammetry. Theory and Applications, Springer-Verlag Berlin Heidelberg New York.

Palazzo, D., Friedmann, R., Nadal, C., Santos Filho, M., Veiga L. and Faggion, P. (2006). Dynamic monitoring of structures using a robotic total station, Proceedings of the 13<sup>th</sup> FIG Congress Shape the Change.

Roncella, R., Forlani, G., and Pinto, L. (2008). Photogrammetric Survey of Ancients Musical Instruments, The International Archives of Photogrammetry and Remote Sensing, Vol. XXXVII, part B5, 309-314.

Tsan-Wing, NG., and Kin-Wah, L. (2001). Deformation survey for the preservation of lei Cheng Uk Han tomb. Proceeding of the 10<sup>th</sup> FIG International Symposium on Deformation Measurements, 294-301.

Yilmazturk, F., Kulur, S., Terzib, N. (2008). Determination of displacements in load tests with digital multimedia photogrammetry, The International Archives of Photogrammetry and Remote Sensing, Vol. XXXVII, part B5, pp. 719-721.

## BIOGRAPHICAL NOTES

Benedetto Villa is full Professor of Geomatics at the Faculty of Architecture of Palermo University. Till 2010 he did his own research work at Department of Representation of which he was Head from 2004 to 2010. Since 2011 he is member of Department of Civil, Environmental and Aerospace Engineering. He is member of the *Italian Society of Photogrammetry and Topography* and he was President of the Palermo Section from 1998 to 2002. He was Director of the PhD course in *Sciences of Survey and Representation* at Palermo University. From 2008 to 2011 he was President of the *Italian Association of Professors of Geomatics*. Since 2003 he is Director of the e-learning *Geographical Information System* degree course. He is Director of the *Lab for survey, management and enjoyment of cultural heritage with advanced information technologies* belonging to the Palermo University Lab System and member of the Technical Organizing Committee. At present he is Director of Master course in *Advanced techniques of survey, representation and diagnostics for preservation and fruition of cultural heritage*. He has been and is still Manager of several topographic and photogrammetric surveys carried out by his Department on behalf of public bodies. His research work, mostly developed through programs financed by Ministry of University and Scientific Research, has involved almost all the fields of Geomatics, with particular reference to the applications concerning the sector of cultural heritage. In this regard he has produced till now 130 papers, a lot of which presented during national and international seminars and congresses.

## CONTACTS

Prof. Benedetto Villa  
Department of Civil, Environmental and Aerospace Engineering, University of Palermo  
Viale delle Scienze - Edificio 8  
90128 Palermo  
Italy  
Tel. +3909123896223  
Fax +39091588853  
Email: [benedetto.villa@unipa.it](mailto:benedetto.villa@unipa.it)